Spin Dynamics and Unconventional Coulomb Phase in $Nd_2Zr_2O_7$

M. Léger,[1,2] E. Lhotel,[1,*] M. Ciomaga Hatnean,[3] J. Ollivier,[4] A. R. Wildes,[4] S. Raymond,[5] E. Ressouche,[5] G. Balakrishnan,[3] and S. Petit[2,†]

[1]*Institut Néel, CNRS and Université Grenoble Alpes, 38000 Grenoble, France*
[2]*Laboratoire Léon Brillouin, Université Paris-Saclay, CNRS, CEA, CE-Saclay, F-91191 Gif-sur-Yvette, France*
[3]*Department of Physics, University of Warwick, Coventry CV4 7AL, United Kingdom*
[4]*Institut Laue Langevin, F-38042 Grenoble, France*
[5]*Université Grenoble Alpes, CEA, IRIG, MEM, MDN, 38000 Grenoble, France*

(Received 26 November 2020; revised 15 April 2021; accepted 17 May 2021; published 16 June 2021)

We investigate the temperature dependence of the spin dynamics in the pyrochlore magnet $Nd_2Zr_2O_7$ by neutron scattering experiments. At low temperature, this material undergoes a transition towards an "all-in–all-out" antiferromagnetic phase and the spin dynamics encompass a dispersionless mode, characterized by a dynamical spin ice structure factor. Unexpectedly, this mode is found to survive above $T_N \approx 300$ mK. Concomitantly, elastic correlations of the spin ice type develop. These are the signatures of a peculiar correlated paramagnetic phase which can be considered as a new example of Coulomb phase. Our observations near T_N do not reproduce the signatures expected for a Higgs transition, but show reminiscent features of the "all-in–all-out" order superimposed on a Coulomb phase.

DOI: 10.1103/PhysRevLett.126.247201

Geometrical frustration is well known to be one of the key ingredients leading to unconventional states of matter, especially in magnetism [1,2]. Among them, spin ice and more generally Coulomb phases [3] have attracted significant interest. These can be considered as an original state of matter formed by disordered degenerate configurations where local degrees of freedom remain strongly constrained at the local scale by an organizing principle. In the case of spin ice, these degrees of freedom are Ising spins, sitting on the sites of a pyrochlore lattice formed of corner sharing tetrahedra and aligned along the axes which connect the corners of the tetrahedra to their center. The organizing principle, the "ice rule," states that each tetrahedron should have two spins pointing in and two out, in close analogy with the rule which controls the hydrogen position in water ice [4]. Importantly, the idea that this local constraint can be considered as the conservation law of an "emergent" magnetic flux ($\nabla \cdot \mathbf{B} = 0$) was quickly imposed [5–7]. Quantum fluctuations can cause this flux to change with time, giving rise to an emergent electric field, and eventually to an emergent quantum electromagnetism [8–10]. This quantum spin ice state hosts spinon (monopole in the spin ice language [11]) and photonlike excitations. Despite much work, however, experimental evidence for this enigmatic physics remains elusive, with the possible exception of $Pr_2Hf_2O_7$ [12]. Indeed, the conditions for the realization of this so-called quantum spin ice state are drastic: transverse terms have to be sizable in the Hamiltonian to enable fluctuations out of the local Ising axes, but should remain small enough to prevent the stabilization of classical phases, called Higgs phases, characterized by ordered components perpendicular to these axes [11,13,14].

The pyrochlore material $Nd_2Zr_2O_7$ offers the opportunity to approach this issue. Recent studies suggest that below 1 K this compound hosts a correlated state, which could be a remarkable novel example of the Coulomb phase [15,16]. This phase would be described by a "two-in–two-out" rule as in spin ice, but built on a pseudospin component different from the conventional $\langle 111 \rangle$ Ising one. The "all-in–all-out" (AIAO) ordering previously observed below $T_N \approx 300$ mK [17,18] would then correspond to the pseudospin ordering in directions perpendicular to the components responsible for the "high temperature" Coulomb phase. It was proposed that a Higgs mechanism may account for this transition [16]. Such a process is invoked in $U(1)$ quantum spin liquids when the deconfined spinon excitations undergo a Bose-Einstein condensation, resulting in a Higgs phase along with a gapped photon excitation [13,19,20].

In this Letter, we show that the paramagnetic phase of $Nd_2Zr_2O_7$ does carry elastic spin icelike correlations, and thus confirm the proposed Coulomb phase picture above T_N. We present a detailed study of the spin dynamics as a function of temperature and explore the nature of this Coulomb phase above and close to the transition. The spin excitations of $Nd_2Zr_2O_7$ deep in the AIAO phase include a peculiar spectrum with a flat band at the energy $E_0 \approx 70\ \mu$eV characterized by a spin icelike $\mathbf{Q}$ dependence [15,21,22]. Using neutron scattering experiments, we report the temperature dependence of the gap E_0, and reveal that this gap persists above T_N. This result is robust,

and withstands a small substitution at the Zr site. The spectra recorded above T_N do not show the spinon continuum expected in the Higgs scenario. Instead, we observe dispersive features reminiscent of the AIAO ordered phase superimposed on the Coulomb phase signal. This coexistence suggests that a strong exchange competition is at work in this temperature range, emphasizing the originality of the Coulomb phase above the transition.

The single crystal samples used in this work are the same as in our previous studies (labeled No. 1 [15,17,21] and No. 2 [21]). In addition, results on a single crystal of $Nd_2(Zr_{1-x}Ti_x)_2O_7$, with $x = 2.4\%$ (sample No. 3) (see Supplemental Material [23]) are presented, not in order to analyze the role of disorder but to illustrate the robustness of the results. Magnetic properties were measured in very low temperature SQUID magnetometers developed at the Institut Néel [29]. The composition and magnetic structure at low temperature were determined using the D23 (CEA-CRG@ILL) neutron diffractometer [23]. Polarized neutron scattering experiments were carried out at D7 (ILL) on sample No. 1. Inelastic neutron scattering (INS) experiments were carried out on the IN5 (ILL) time-of-flight spectrometer on all samples and on the triple axis spectrometer IN12 (CEA-CRG@ILL) for sample No. 1. The INS data have been analyzed using the CEFWAVE software developed at LLB.

The XYZ Hamiltonian proposed to describe the properties of Nd based pyrochlores due to the peculiar dipolar-octupolar character of the Nd^{3+} ion [30], writes

$$\mathcal{H} = \sum_{\langle i,j \rangle} [\mathsf{J}_x \tau_i^x \tau_j^x + \mathsf{J}_y \tau_i^y \tau_j^y + \mathsf{J}_z \tau_i^z \tau_j^z + \mathsf{J}_{xz}(\tau_i^x \tau_j^z + \tau_i^z \tau_j^x)]. \quad (1)$$

In this Hamiltonian, τ_i is not the actual spin, but a pseudospin which resides on the rare-earth sites of the pyrochlore lattice. Its z component relates to the usual magnetic moment and is directed along the local $\langle 111 \rangle$ directions of the tetrahedra of the pyrochlore lattice. This Hamiltonian can be rewritten by rotating the $\mathbf{x}$ and $\mathbf{z}$ axes in the $(\mathbf{x}, \mathbf{z})$ plane by an angle θ. In this $(\tilde{\mathbf{x}}, \tilde{\mathbf{z}})$ rotated frame, the relevant parameters of the Hamiltonian $\mathcal{H}$ are labeled $\tilde{\mathsf{J}}_{x,y,z}$, leading to [30,31]

$$\mathcal{H}_{XYZ} = \sum_{\langle i,j \rangle} [\tilde{\mathsf{J}}_x \tilde{\tau}_i^{\tilde{x}} \tilde{\tau}_j^{\tilde{x}} + \tilde{\mathsf{J}}_y \tilde{\tau}_i^{\tilde{y}} \tilde{\tau}_j^{\tilde{y}} + \tilde{\mathsf{J}}_z \tilde{\tau}_i^{\tilde{z}} \tilde{\tau}_j^{\tilde{z}}]$$

$$\text{with} \quad \tan(2\theta) = \frac{2\mathsf{J}_{xz}}{\mathsf{J}_x - \mathsf{J}_z}. \quad (2)$$

With time and maturation of the subject, the estimated parameters for $Nd_2Zr_2O_7$ have evolved. Determinations of the $\tilde{\mathsf{J}}_i$ parameters are based on the spin wave spectra measured at very low temperature in zero field [15,22,31] or applied field [21], while the angle θ is deduced from the Curie-Weiss temperature [31] and/or the ordered AIAO magnetic moment [21,22]. The sets of reported parameters are summarized in Table I, where we have added the parameters refined here for the $Nd_2(Zr_{1-x}Ti_x)_2O_7$ sample (sample No. 3) [23] and have revisited the ones of samples No. 1 and No. 2. From these values, two interesting features stand out, which remain unexplained to date and should be further explored to ascertain their relevance: (i) the larger the Néel temperature, the larger the ordered moment along $\mathbf{z}$ is; (ii) very similar $\tilde{\mathsf{J}}_i$ parameters are obtained for the various samples, despite differences with regard to the amount of impurities or to the ordering parameters.

The J parameters lead to an ordered AIAO ground state, where the pseudospins point along the (local) direction $\tilde{\mathbf{z}}$, turned around the $\mathbf{z}$ axis towards the $\mathbf{x}$ axis by the angle θ [31]. As shown by INS experiments, peculiar excitations are associated with this ground state. They manifest as an inelastic spin icelike flat mode at an energy $E_0 \approx 70$ μeV, above which spin wave branches disperse [see Fig. 4(a) for sample No. 1] [15]. This excitation spectrum is understood in the framework of the *dynamic fragmentation* [31,32] as the sum of a dynamic divergence-free contribution, giving rise to the flat mode at E_0 and of a dynamic curl-free contribution, which takes the form of the dispersing branches. These spin waves correspond to the propagation of magnetically charged excitations and have a spectral weight made of half-moons in reciprocal space [15,33].

Instantaneous spin-spin correlations $S(\mathbf{Q})$ were measured in sample No. 1 as a function of temperature between 60 mK and 1 K through polarized neutron scattering

TABLE I. Ordered moment m_{ord} along $\mathbf{z}$, transition temperature T_N, and Hamiltonian parametrization reported in different studies. $\tilde{\mathsf{J}}_i$ parameters for sample No. 1 and from Ref. [31] were obtained from fits of the INS data reported in Ref. [15] and, for sample No. 2 in Ref. [21]. m_{ord} from Ref. [31] is a calculated value. The total Nd^{3+} magnetic moment is estimated to ≈ 2.4 μ_B [17,18].

Sample or Ref.	m_{ord} (μ_B)	T_N (mK)	Hamiltonian parameters (K)				θ (rad)
			$\tilde{\mathsf{J}}_x$	$\tilde{\mathsf{J}}_y$	$\tilde{\mathsf{J}}_z$	$\tilde{\mathsf{J}}_x/\lvert\tilde{\mathsf{J}}_z\rvert$	
No. 1	0.8 ± 0.05	285	1.18	−0.03	−0.53	2.20	1.23
No. 2	1.1 ± 0.1	340	1.0	0.066	− 0.5	2.0	1.09
No. 3	1.19 ± 0.03	375	0.97	0.21	−0.53	1.83	1.08
[22]	1.26	400	1.05	0.16	−0.53	1.98	0.98
[31]	1.4		1.2	0.0	−0.55	2.18	0.83

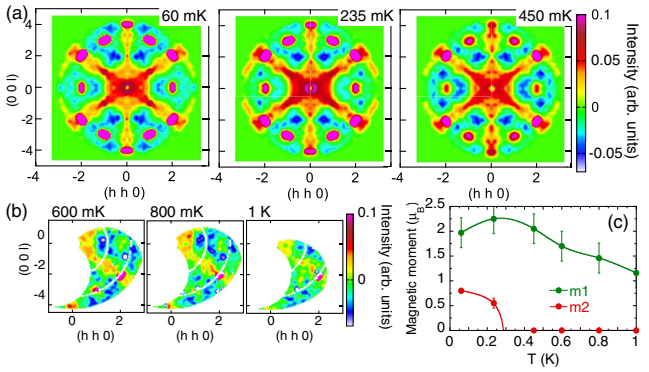

FIG. 1. (a),(b) Magnetic instantaneous correlations in sample No. 1 as a function of temperature. The 10 K dataset has been subtracted as a background reference. Measurements in (a) were symmetrized. (c) "Spin ice" moment m_1 and AIAO ordered moment m_2 along $\mathbf{z}$ as a function of temperature [23]. Lines are guides to the eye.

experiments and are displayed in Fig. 1 [23]. These measurements integrate over the neutron energy loss up to 3.5 meV, and thus contain both elastic and inelastic signals. At 1 K, a spin ice pattern can barely be observed, revealing the onset of a Coulomb phase. Upon cooling, the spin ice pattern becomes clearly visible below 600 mK. At 450 mK, the magnetic moment m_1 responsible for the spin icelike diffuse scattering is estimated to $2.05 \pm 0.3\ \mu_B$ [23], to be compared to the 2.4 μ_B full Nd moment [17,18]. In addition to this signal, below 800 mK, magnetic diffuse scattering spots appear around (220), (113), and symmetry related positions. Intensity on these positions increases with cooling until they transform into Bragg peaks below T_N (285 mK in this sample) characteristic of the AIAO phase. At low temperature, the corresponding ordered magnetic moment is $m_2 = m_{\mathrm{ord}} = 0.8 \pm 0.05\ \mu_B$ (from diffraction measurements) and the magnetic contribution to the spin icelike diffuse scattering amounts to $m_1 = 2 \pm 0.3\ \mu_B$ [23] [see Fig. 1(c)]. The moment embedded in the spin ice correlations is thus at maximum around T_N and slightly decreases at lower temperature. The diffuse scattering observed in the vicinity of the Bragg peak positions above T_N might arise from AIAO diffuse scattering just above the ordering transition, but could also be a signature of deconfined excitations, as proposed in Ref. [16].

To determine the spectral profile contained in those magnetic correlations, and especially the elastic or inelastic nature of the spin ice correlations associated with m_1, INS measurements have been carried out on the three aforementioned samples (see Table I) as a function of temperature. To highlight the possible presence of an inelastic flat mode, the $\mathbf{Q}$-integrated spectral function $S(E) = \int d\mathbf{Q} S(\mathbf{Q}, E)$ was computed. As this quantity is akin to a density of states, it enhances the contribution of the flat modes contained in the spectrum. Figure 2 displays $S(E)$ at different temperatures. As previously shown [15], the

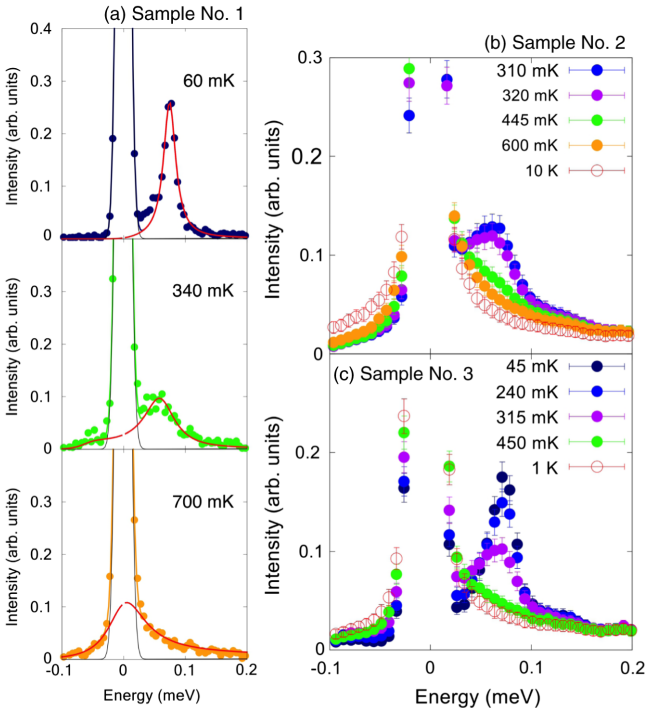

FIG. 2. Spectral function $S(E)$ at different temperatures [23] measured at a wavelength $\lambda = 8.5$ Å, hence an energy resolution of 20 μeV: (a) in sample No. 1, integrated around $\mathbf{Q} = (0.8\,0.8\,0.8)$. The grey and red lines correspond to the fitted incoherent elastic I_c and inelastic S_0 contributions, respectively. (b) and (c): integrated over the measured $\mathbf{Q}$ range in samples No. 2 (b) and No. 3 (c).

inelastic flat band is clearly seen at low temperature. It is still visible at finite energy close to T_N (320 mK for sample No. 2 and 315 mK for sample No. 3) and above T_N (340 mK for sample No. 1), yet broadens significantly upon warming. At the highest temperatures, the signal looks almost quasielastic. To obtain a quantitative insight into the temperature evolution of the mode, data were fitted for the three samples [as shown in Fig. 2(a) for sample No. 1] to the following model [23]:

$$S(E) = b + I_c(E) + F(E,T) \times [S_0(E) + S_1(E)], \quad (3)$$

b is a flat background, $I_c(E)$ is a Gaussian function centered at zero energy to account for the elastic incoherent scattering. $F(E,T) = 1 + n(E,T)$ is the detailed balance factor (n is the Bose-Einstein distribution). $S_0(E)$ and $S_1(E)$ are two Lorentzian profiles, centered on the energy $E_{0,1}$ and of intensity $I_{0,1}$, which represent, respectively, the flat band and the dispersive mode typical of the spin wave spectrum in $Nd_2Zr_2O_7$.

The determined positions E_0 and intensities I_0 are shown in Fig. 3 as a function of the temperature normalized to T_N for the three samples. As anticipated from Fig. 2, with increasing temperature, the band at E_0 softens and broadens while its intensity decreases. Nevertheless, E_0 is nonzero at

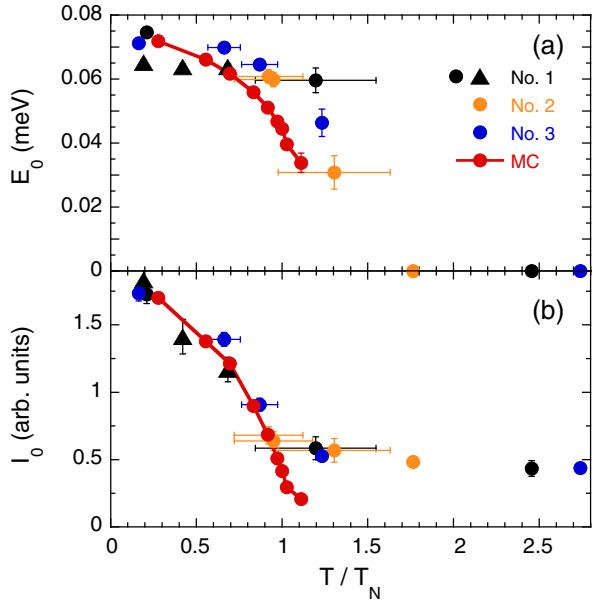

FIG. 3. (a) E_0 and (b) I_0 as a function of reduced temperature T/T_N obtained from measurements on IN5 (dots—see Fig. 2) and IN12 (triangles), together with results from Monte Carlo (MC) calculations from Ref. [16] (red dots) [23]. Lines are guides to the eye. The large I_0 experimental value when $E_0 = 0$ is the signature of the persistent quasielastic contribution above T_N.

T_N and a persistent dynamical behavior is observed in all samples at and above T_N, up to about $2T_N$. Finally, the width of the features above the flat mode makes it hard to extract quantitative information from S_1. However, close examination of $S(\mathbf{Q}, E)$ measured for sample No. 1 above T_N at 340 mK (see Fig. 4) shows that, in all investigated directions, besides a strong quasielastic contribution (the inelastic mode being hardly discernible due to the energy resolution and the color scale), weak features are present close to the position of the low temperature dispersions. These spin wave fingerprints, highlighted by arrows on Fig. 4(b) and which manifest as a broad signal in $\mathbf{Q}$ cuts [Figs. 4(c) and 4(d)], are not compatible with the excitation spectrum expected in the presence of monopole creation and hopping [16].

Several striking features emerge from these measurements. INS experiments reveal that the intensity I_0 of the inelastic spin ice mode decreases when increasing temperature. Since D7 polarized experiments show that the full spin ice correlations, elastic and inelastic, are strongest around T_N, the spin ice pattern observed above T_N must contain a new spin ice contribution, likely elastic, and different from the inelastic mode at E_0. This is confirmed by magnetization measurements, which point to ferromagneticlike correlations, as expected for spin ice [23]. This elastic signal could not be directly identified in the elastic line of the IN5 data [23] certainly due to background issues, but we should stress that the D7 polarization analysis is definitely the most appropriate way to remove properly nuclear contributions and visualize small magnetic contributions. These results thus point to the coexistence of *two* spin icelike contributions, an elastic and an inelastic one with different origins, and different temperature dependences.

These two contributions can be understood as the manifestation of the strong competition at play between the pseudospin components of Nd. The negative value of $\tilde{J}_z$ (see Table I) promotes an AIAO phase built on $\tilde{\tau}^{\tilde{z}}$ while the positive $\tilde{J}_x$ favors a Coulomb phase, similar to a spin ice phase, but built on $\tilde{\tau}^{\tilde{x}}$. For $\tilde{J}_x/|\tilde{J}_z| \approx 2$, the value determined for $Nd_2Zr_2O_7$, the former is stabilized at low temperature and the latter at finite temperature, due to the large entropy associated to the Coulomb phase. In these two regimes, spin ice contributions are expected, an *elastic* one in the Coulomb phase at "high" temperature, and an *inelastic* one in the AIAO ordered phase (accompanied by dispersive excitations). Remarkably, the observable τ_z, which corresponds to the magnetic dipolar moment along the local

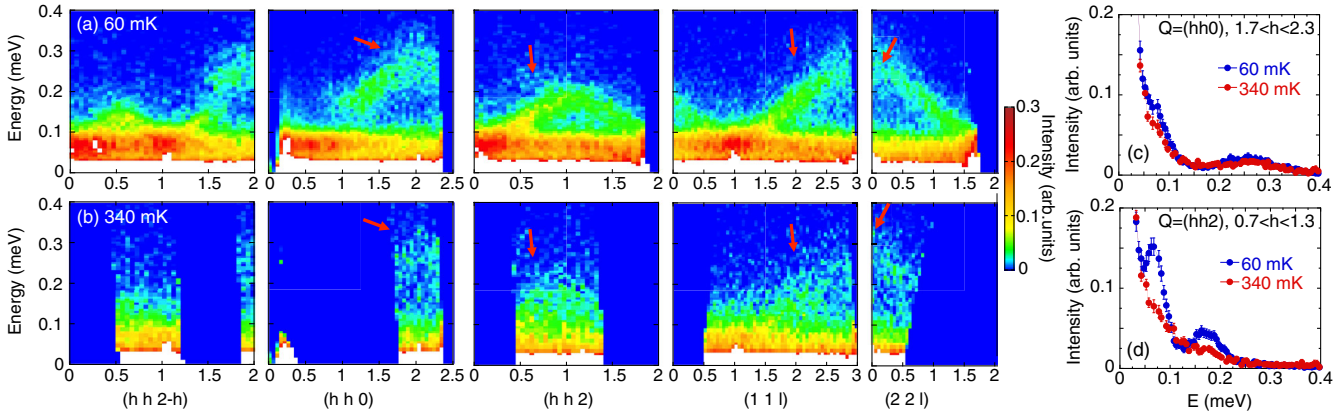

FIG. 4. INS spectra of sample No. 1 along several high symmetry directions at 60 mK (a) and 340 mK (b), measured on IN5 with $\lambda = 6$ Å. Red arrows highlight the dispersive modes and their fingerprints above T_N. (c),(d) Constant $\mathbf{Q}$ cuts at these two temperatures, integrated (c) along $(hh0)$ and (d) along $(hh2)$.

$\langle 111 \rangle$ axes, is a combination of the $\tilde{\tau}^{\tilde{x}}$ and $\tilde{\tau}^{\tilde{z}}$ components of the pseudospin. It thus holds the two competing contributions (AIAO and Coulomb), which contrasts with the conventional spin ice case where the z component carries elastic spin ice correlations only.

The present results shed light on the manner in which the system evolves from the high temperature Coulomb phase to the low temperature AIAO ordered phase. At high temperature, around 1 K, the elastic spin ice signal characteristic of the $\tilde{\tau}^{\tilde{x}}$ Coulomb phase appears first. Upon cooling, the inelastic spin ice contribution along with dispersive spin wave branches emerge above T_N and coexist with the elastic one. They can naturally be considered as excitations stemming from the short-range AIAO correlations of the $\tilde{\tau}^{\tilde{z}}$ component observed below 800 mK (see Fig. 1).

The system enters the long-range AIAO ordered state at a temperature $T_N \approx 300$ mK. It corresponds to about $|\tilde{J}_x|/4$, thus to a temperature scale far above the one obtained theoretically for the stabilization of the quantum regime of spin ice, which is estimated to a few percents of the characteristic exchange interaction [34,35]. This indicates that the Coulomb phase remains in its thermal regime down to T_N. Surprisingly, the ordering temperature is larger than semiclassical Monte Carlo calculations predictions [16]. At T_N, the excitation spectrum is gapped, with the coexistence between the elastic spin ice component and the inelastic spectrum typical of AIAO ordering. The lack of a spinon continuum which would condense at T_N seems to preclude a transition driven by a Higgs mechanism.

Deeper in the AIAO phase, the inelastic component—together with the Bragg peaks—develops at the expense of the elastic component. The weak maximum of the spin ice m_1 moment around T_N can thus be interpreted as due to the rise of the inelastic spin ice mode along with the persistence of the elastic contribution of the Coulomb phase. The coexistence of the elastic and inelastic signals is consistent with MC calculations [16], even if, close to T_N, the two modes are less distinguishable in the experiments than in the calculations due to the strong broadening of the inelastic mode. Although some distribution is observed between the samples, the measured temperature dependence of the inelastic spin ice mode, described by the energy $E_0(T)$ and intensity $I_0(T)$, is also consistent with calculations [23], despite a slightly stronger inelastic component in experiments above T_N (see Fig. 3).

In summary, we find that with increasing temperature, the now well-established flat spin ice band characteristic of the AIAO ground state in $Nd_2Zr_2O_7$, softens while its intensity decreases. The energy of this mode remains however finite at and above T_N and becomes overdamped with increasing the temperature further. At the same time, a new elastic spin ice component appears. The nature of the correlated phase above T_N is thus highly unconventional with the coexistence of an (elastic) Coulomb phase and fragmented excitations, resulting from the competition between the different terms of the Hamiltonian. Our observations support a picture where the AIAO ordering arises from a thermal spin ice phase, a scenario which is well accounted for by semiclassical MC calculations from Ref. [16], and is different from the proposed Higgs transition. When increasing the ratio $\tilde{J}_x/|\tilde{J}_z|$, reentrant behaviors are predicted [16] while the system approaches a quantum spin liquid ground state [31]. Tuning the parameters of the Hamiltonian (2) with novel materials would thus be of high interest to understand the unusual behavior of $Nd_2Zr_2O_7$ and explore the frontiers between thermal and quantum regimes.

The work at the University of Warwick was supported by EPSRC, UK through Grant No. EP/T005963/1. M. L. and S. P. acknowledge financial support from the French Federation of Neutron Scattering (2FDN). M. L. acknowledges financial support from Université Grenoble-Alpes (UGA). M. L., E. L., and S. P. acknowledge financial support from ANR, France, Grant No. ANR-19-CE30-0040-02. S. P. and E. L. acknowledge F. Damay for helpful remarks and J. Xu for providing the data of his calculations. E. L. acknowledges C. Paulsen for the use of his magnetometers.

*elsa.lhotel@neel.cnrs.fr
†sylvain.petit@cea.fr

[1] *Introduction to Frustrated Magnetism*, edited by C. Lacroix, P. Mendels, and F. Mila (Springer-Verlag, Berlin, 2011).
[2] J. S. Gardner, M. J. P. Gingras, and J. E. Greedan, Magnetic pyrochlore oxides, Rev. Mod. Phys. **82**, 53 (2010).
[3] C. L. Henley, The "Coulomb phase" in frustrated systems, Annu. Rev. Condens. Matter Phys. **1**, 179 (2010).
[4] M. J. Harris, S. T. Bramwell, D. F. McMorrow, T. Zeiske, and K. W. Godfrey, Geometrical Frustration in the Ferromagnetic Pyrochlore $Ho_2Ti_2O_7$, Phys. Rev. Lett. **79**, 2554 (1997).
[5] S. V. Isakov, K. Gregor, R. Moessner, and S. L. Sondhi, Dipolar Spin Correlations in Classical Pyrochlore Magnets, Phys. Rev. Lett. **93**, 167204 (2004).
[6] C. L. Henley, Power-law spin correlations in pyrochlore antiferromagnets, Phys. Rev. B **71**, 014424 (2005).
[7] C. Castelnovo, R. Moessner, and S. L. Sondhi, Magnetic monopoles in spin ice, Nature (London) **451**, 42 (2008).
[8] M. Hermele, M. P. A. Fisher, and L. Balents, Pyrochlore photons: The $U(1)$ spin liquid in a $S = 1/2$ three-dimensional frustrated magnet, Phys. Rev. B **69**, 064404 (2004).
[9] N. Shannon, O. Sikora, F. Pollmann, K. Penc, and P. Fulde, Quantum Ice: A Quantum Monte Carlo Study, Phys. Rev. Lett. **108**, 067204 (2012).
[10] O. Benton, O. Sikora, and N. Shannon, Seeing the light: Experimental signatures of emergent electromagnetism in a quantum spin ice, Phys. Rev. B **86**, 075154 (2012).

[11] M. J. P. Gingras and P. A. McClarty, Quantum spin ice: A search for gapless quantum spin liquids in pyrochlore magnets, Rep. Prog. Phys. **77**, 056501 (2014).
[12] R. Sibille, N. Gauthier, H. Yan, M. Ciomaga Hatnean, J. Ollivier, B. Winn, G. Balakrishnan, M. Kenzelmann, N. Shannon, and T. Fennell, Experimental signatures of emergent quantum electrodynamics in a quantum spin ice, Nat. Phys. **14**, 711 (2018).
[13] L. Savary and L. Balents, Coulombic Quantum Liquids in Spin-1/2 Pyrochlores, Phys. Rev. Lett. **108**, 037202 (2012).
[14] Z. Hao, A. G. R. Day, and M. J. P. Gingras, Bosonic many-body theory of quantum spin ice, Phys. Rev. B **90**, 214430 (2014).
[15] S. Petit, E. Lhotel, B. Canals, M. Ciomaga Hatnean, J. Ollivier, H. Mutka, E. Ressouche, A. R. Wildes, M. R. Lees, and G. Balakrishnan, Observation of magnetic fragmentation in spin ice, Nat. Phys. **12**, 746 (2016).
[16] J. Xu, O. Benton, A. T. M. N. Islam, T. Guidi, G. Ehlers, and B. Lake, Order Out of a Coulomb Phase and Higgs Transition: Frustrated Transverse Interactions in $Nd_2Zr_2O_7$, Phys. Rev. Lett. **124**, 097203 (2020).
[17] E. Lhotel, S. Petit, S. Guitteny, O. Florea, M. Ciomaga Hatnean, C. Colin, E. Ressouche, M. R. Lees, and G. Balakrishnan, Fluctuations and All-In-All-Out Ordering in Dipole-Octupole $Nd_2Zr_2O_7$, Phys. Rev. Lett. **115**, 197202 (2015).
[18] J. Xu, V. K. Anand, A. K. Bera, M. Frontzek, D. L. Abernathy, N. Casati, K. Siemensmeyer, and B. Lake, Magnetic structure and crystal-field states of the pyrochlore antiferromagnet $Nd_2Zr_2O_7$, Phys. Rev. B **92**, 224430 (2015).
[19] D. Pekker and C. M. Varma, Amplitude/Higgs modes in condensed matter physics, Annu. Rev. Condens. Matter Phys. **6**, 269 (2015).
[20] L.-J. Chang, S. Onoda, Y. Su, Y.-J. Kao, K.-D. Tsuei, Y. Yasui, K. Kakurai, and M. R. Lees, Higgs transition from a magnetic Coulomb liquid to a ferromagnet in $Yb_2Ti_2O_7$, Nat. Commun. **3**, 992 (2012).
[21] E. Lhotel, S. Petit, M. Ciomaga Hatnean, J. Ollivier, H. Mutka, E. Ressouche, M. R. Lees, and G. Balakrishnan, Evidence for dynamic kagome ice, Nat. Commun. **9**, 3786 (2018).
[22] J. Xu, O. Benton, V. K. Anand, A. T. M. N. Islam, T. Guidi, G. Ehlers, E. Feng, Y. Su, A. Sakai, P. Gegenwart, and B. Lake, Anisotropic exchange hamiltonian, magnetic phase diagram, and domain inversion of $Nd_2Zr_2O_7$, Phys. Rev. B **99**, 144420 (2019).
[23] See Supplemental Material at http://link.aps.org/supplemental/10.1103/PhysRevLett.126.247201 for details on single crystal growth, neutron diffraction, polarized neutron experiments, inelastic neutron experiments, spin dynamics in Ti doped sample, analysis of classical dynamics results, magnetization, which includes Refs. [24–28].
[24] M. Ciomaga Hatnean, M. R. Lees, and G. Balakrishnan, Growth of single-crystals of rare-earth zirconate pyrochlores, $Ln_2Zr_2O_7$ (with Ln = La, Nd, Sm, and Gd) by the floating zone technique, J. Cryst. Growth **418**, 1 (2015).
[25] M. Ciomaga Hatnean, C. Decorse, M. R. Lees, O. A. Petrenko, and G. Balakrishnan, Zirconate pyrochlore frustrated magnets: crystal growth by the floating zone technique, Crystals **6**, 79 (2016).
[26] J. Rodríguez-Carvajal, Recent advances in magnetic structure determination by neutron powder diffraction, Physica (Amsterdam) **192B**, 55 (1993).
[27] O. Arnold *et al.*, Mantid—data analysis and visualization package for neutron scattering and μSR experiments, Nucl. Instrum. Methods Phys. Res., Sect. A **764**, 156 (2014).
[28] R. A. Ewings, A. Buts, M. D. Lee, J. van Duijn, I. Bustinduy, and T. G. Perring, Horace: Software for the analysis of data from single crystal spectroscopy experiments at time-of-flight neutron instruments, Nucl. Instrum. Methods Phys. Res., Sect. A **834**, 132 (2016).
[29] C. Paulsen, Dc magnetic measurements, in *Introduction to Physical Techniques in Molecular Magnetism: Structural and Macroscopic Techniques—Yesa 1999*, edited by F. Palacio, E. Ressouche, and J. Schweizer (Servicio de Publicaciones de la Universidad de Zaragoza, Zaragoza, 2001), p. 1.
[30] Y.-P. Huang, G. Chen, and M. Hermele, Quantum Spin Ices and Topological Phases from Dipolar-Octupolar Doublets on the Pyrochlore Lattice, Phys. Rev. Lett. **112**, 167203 (2014).
[31] O. Benton, Quantum origins of moment fragmentation in $Nd_2Zr_2O_7$, Phys. Rev. B **94**, 104430 (2016).
[32] M. E. Brooks-Bartlett, S. T. Banks, L. D. C. Jaubert, A. Harman-Clarke, and P. C. W. Holdsworth, Magnetic-Moment Fragmentation and Monopole Crystallization, Phys. Rev. X **4**, 011007 (2014).
[33] H. Yan, R. Pohle, and N. Shannon, Half moons are pinch points with dispersion, Phys. Rev. B **98**, 140402(R) (2018).
[34] L. Savary and L. Balents, Spin liquid regimes at nonzero temperature in quantum spin ice, Phys. Rev. B **87**, 205130 (2013).
[35] C.-J. Huang, Y. Deng, Y. Wan, and Z. Y. Meng, Dynamics of Topological Excitations in a Model Quantum Spin Ice, Phys. Rev. Lett. **120**, 167202 (2018).